International Journal of Ethics in Engineering & Management Education
Website: www.ijeee.in (ISSN: 2348-4748, Volume 9, Issue 8, August 2022)

Digital Signal Processing for Coherent Optical Fiber Communications

T. Krishnarjuna Rao
Associate Professor, Dept of ECE
Siddhartha Institute of Engineering and Technology
Ibrahimpatnam, Hyderabad

G. Suman
Assistant Professor, Dept of ECE
Sri Indu Institute of Engineering & Technology
Ibrahimpatnam, Hyderabad

Abstract: **In this postulation examinations were performed into advanced sign handling (DSP) calculations for reasonable optical fiber transmission frameworks, which furnish enhanced execution concerning customary frameworks and calculations. Firstly, a review of sound identification and intelligible transmission frameworks is given. Exploratory examinations were then performed into the execution of computerized back proliferation for alleviating fiber nonlinearities in a double polarization quadrature stage shift keying (DP-QPSK) framework more than 7780 km and a double polarization 16-level quadrature abundancy tweak (DP-QAM16) framework more than 1600 km. It is noticed that critical enhancements in execution might be accomplished for a nonlinear step-size more noteworthy than one compass. An around exponential relationship was found between execution change in Q-component and the number for required complex multipliers. DSP calculations for polarization-exchanged quadrature stage shift keying (PS-QPSK) are then explored. A novel two-section leveling calculation is proposed which gives peculiarity free merging and dazzle adjustment of PS-QPSK. This calculation is described and its application to wavelength division multiplexed (WDM) transmission frameworks is talked about.**

Keywords: **ADC, ASE, ASIC, Local oscillator, Gigabit Ethernet, Bit mistake rate, Chromatic scattering.**

1. INTRODUCTION

The conception of optical fiber correspondences frameworks in the mid 1970s delivered a dangerous development in information transfers with the presentation of low misfortune, high data transmission silica filaments [1]. Increments in line rates in these early frameworks were accomplished basically by expanding the regulation rate of on-off keyed (OOK) signals as image rates expanded, frameworks were restricted by the misfortune that could be endured before electrical recovery was required. At this stage, lucid discovery was initially explored as a strategy for expanding the affectability of optical recipients [3]. While a change in affectability of up to 20 dB was accomplished, reasonable recognition was superseded with the creation of the optical fiber enhancer [4].

Erbium doped fiber speakers (EDFAs) give intensification in the optical space, giving THz of addition transmission capacity, empowering enhancement of a few wavelength channels. Further increments in scope got to be accessible with the creation of backwards scattering strands, permitting optical space pay of chromatic scattering (CD). While optical line rates kept on expanding to many Gb/s, EDFAs empowered a vast increment altogether limit per fiber. This expansion was because of the utilization of a few optical transporters of contrasting wavelengths on a solitary fiber, known as wavelength division multiplexing (WDM) [5]. The bearers are de-multiplexed at the beneficiary with a wavelength specific gadget, for example, an exhibited waveguide grinding (AWG), and identified separately.

Despite the fact that the expansion in limit empowered by EDFAs and WDM has scaled well before, a hard farthest point on limit exists while OOK tweak is utilized, given that the most extreme achievable data phantom thickness (ISD) is 1 b/s/Hz. Amid the advancement of 40 Gb/s transmission frameworks, the need to keep up similarity with the ITU recurrence matrix of 50 GHz for WDM frameworks and diminish the requirement for amazingly high transfer speed electronic segments got to be obvious. Because of these weights, propelled adjustment designs which are fit for transmitting more than one piece for each image (and accordingly an ISD of more than 1 b/s/Hz) turned into a profoundly attractive specialized progression [6]. A few transmission frameworks were executed for 40 Gb/s transmission, two of which depended on quadrature stage shift keying (QPSK). Differential identification of differentially coded QPSK (DQPSK) gives a low optical intricacy arrangement at 40 Gb/s, and depends on self-intelligible discovery utilizing a postponement line interferometer (DLI) and quadrature location [7]. The postponement line interferometer parts the approaching sign into two equivalent segments, one of which is deferred by one image period. The two segments are then recombined in a 2x2 coupler which has yields in quadrature. These optical signs are then distinguished and examined, giving the two bits of data which include the QPSK image. Despite the fact that DQPSK gave a generally cost productive technique for accomplishing 40 Gb/s transmission over a 50 GHz WDM lattice, self-sound discovery has characteristics which restrict the scaling of this innovation to higher line rates. Because of the way that the sign is blended with itself, the change in affectability is not as much as that of full cognizant location. Signs are additionally restricted by straight bends, for example, polarization mode scattering (PMD) and CD which scale directly and with the square of baud rate individually. Extra tweak thickness might be accomplished just with the option of further stage levels and extra DLI structures in the recipient, including cost and

International Journal of Ethics in Engineering & Management Education
Website: www.ijeee.in (ISSN: 2348-4748, Volume 9, Issue 8, August 2022)

multifaceted nature while altogether expanding many-sided quality.

The second QPSK-based answer for 40 Gb/s transmission was completely intelligent identification with computerized post-preparing of double polarization QPSK (DP-QPSK) [8]. Advanced sound identification includes part the approaching sign into two orthogonal straight polarizations, blending the sign with a free-running neighborhood oscillator and performing recognition of the in-stage and quadrature segments for both polarizations. This plan results in recognition of each of the four measurements of the optical field, along these lines saving all data contained in the got signal [9]. After quantisation, twists are expelled from the sign with the utilization of DSP systems, such that the channel is balanced, the polarization states are isolated and the variety in stage and recurrence between the nearby oscillator and source lasers is evacuated. This plan permits the utilization of polarization multiplexing without the requirement for versatile optics, furthermore empowers full remuneration of self-assertive measures of already restricting impacts, for example, PMD and CD [10]. The balance organization of decision for 40 Gb/s with sound location has ended up DP-QPSK, which conveys 4 bits for each image (bringing about an extreme point of confinement of 4 b/s/Hz ISD). The higher regulation thickness results in a lower transmission capacity prerequisite for electrical parts, with only 5 GHz required for most segments alongside 10 GSa/s for the simple to advanced convertors (ADCs).

While advanced lucid recognition requires extra optical parts in correlation to different plans (to be specific the optical half and half, nearby oscillator and extra photograph locators), and along these lines brings about extra cost, both heartiness to mutilation and scaling to higher line-rates are extraordinarily expanded. This might be outlined by the late improvement in 100 Gb/s transmission frameworks. The business standard for 100 Gb/s handsets [11] indicates the utilization of computerized intelligent location in mix with DP-QPSK adjustment. This expansion in bit rate was empowered by basically expanding the data transfer capacity of electrical segments and expanding the inspecting rate of the ADCs to 56 GSa/s. The specialized difficulties included in this scaling were totally in the electrical space. Beforehand restricting optical mutilations, for example, PMD and CD might be completely remunerated without punishment, leaving just nonlinearity as a constraining optical contortion.

2. LITERATURE REVIEW AND THEORY

In this chapter, the basic concepts of coherent detection are discussed. The details of polarization and phase diverse coherent detection are described for both single ended and balanced photo-detection. Local oscillator phase and frequency locking is studied, as are the constraints on analogue to digital conversion. Common modulation formats used for coherent detection are assessed and compared by noise sensitivity. Fibre transmission impairments are discussed, with different mathematical descriptions for fibre with and without chromatic dispersion, polarization mode dispersion, and Kerr nonlinearity. Noise resulting from amplified spontaneous emission in optical amplifiers is also described. Digital post-processing algorithms are then examined. These include: filters for the compensation of chromatic dispersion; adaptive equalization of PMD, polarization rotations and residual filtering; intradyne frequency offset estimation and compensation; and carrier phase estimation. The theoretical basis of nonlinearity compensation with digital back propagation is then reviewed. Back propagation is analysed using two and three block nonlinear models, and step sizes of more than and less than one span. Recent experimental results using digital back propagation are noted, and alternatives to back propagation discussed.

2.1. Characterisation of PS-CMA Performance

An essential capability of any practical equaliser is the ability to operate effectively in the presence of polarization dependant loss (PDL). To characterise the performance of the equaliser in the presence of PDL we took the transmitted optical signal, applied loss at a particular polarization orientation and then noise loaded to 5.8 dB E_b/N_0. We considered the orientation of the loss as a polarization which is circularly rotated with respect to the signal, that is, 9 was varied between -n and n, while ^ remained zero. The signal is then rotated again with respect to the polarization axes of the receiver such that the input state of polarization to the receiver is randomised. The mean Q-factor penalty with respect to the SNR limited optimum was then calculated over the entire polarization space.

2.2. Comparison with Other Published PS-QPSK Algorithms

To-date, only two papers have directly addressed the issue of fully blind equalisation of PS-QPSK. The algorithm used by Nelson et al in [115] is a normalised version of the PS-CMA derived above, although the initialisation algorithm was not used, and so the singularity issue will still be present. This work was done in parallel to and was published shortly after our research, presented in [13] and [15]. An alternative equaliser algorithm was presented in [14] while our work was under review. While the algorithm presented in [14] uses a different control surface to the PS-CMA described above, the operation is remarkably similar. The only significant difference between the two algorithms is the initialisation procedure described in section 4.4, which mitigates the possibility of singular mal-convergence. To compare the performance of the two algorithms, we have simulated the back-to-back performance of both algorithms after a polarization rotation. The simulation was identical to that previously described for Figure.

International Journal of Ethics in Engineering & Management Education
Website: www.ijeee.in (ISSN: 2348-4748, Volume 9, Issue 8, August 2022)

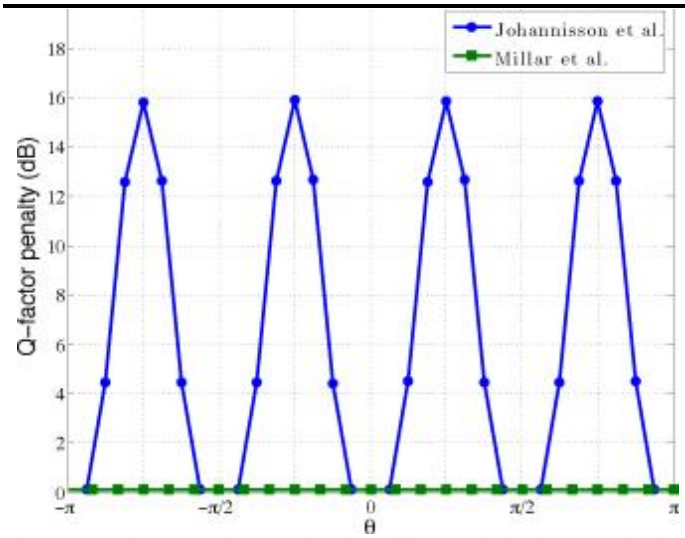

Figure 2 - Q-factor penalty as a function of input polarization state for the equaliser algorithm as described in [14] (Johannisson et al.) compared with that described in section 4.4 (Millar et al.).

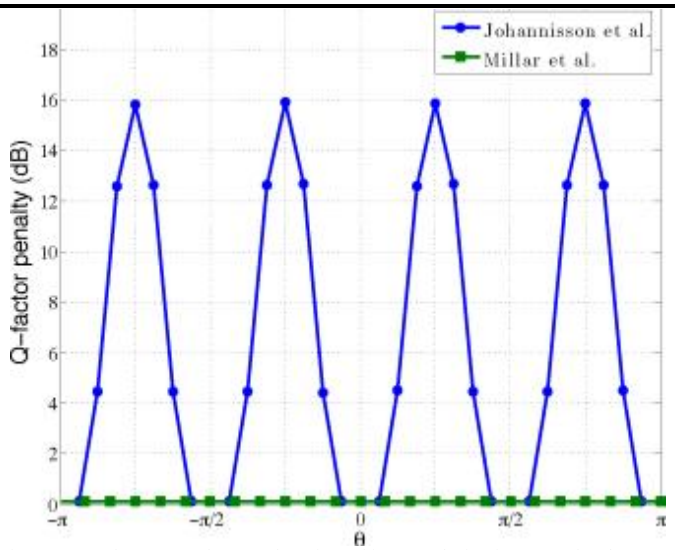

Figure 3 - Q-factor penalty as a function of input polarization state for the equaliser algorithm as described in [14] (Johannisson et al.) compared with that described in section 4.4 (Millar et al.).

We note from Figure 4.13 that while the minimum Q-factor penalty of the equalisers is broadly similar in the optimum case, the algorithm described in [14] (Johannisson et al.) suffers from singular mal-convergence resulting in a high Q-factor penalty. A high penalty is seen for values of 9 of ±n/2 and ±3n/2, which correspond to angles whereby the energy of each signal polarization is evenly distributed onto the two receiver polarizations. This result is in agreement with the previous analysis of the performance of the PS-CMA with and without the initialisation algorithm presented in Figure and demonstrates the improvement in robustness which may be achieved with the initialisation algorithm.

2.3. Comparison with Other Published PS-QPSK Algorithms

To-date, only two papers have directly addressed the issue of fully blind equalisation of PS-QPSK. The algorithm used by Nelson et al in [115] is a normalised version of the PS-CMA derived above, although the initialisation algorithm was not used, and so the singularity issue will still be present. This work was done in parallel to and was published shortly after our research, presented in [13] and [15]. An alternative equaliser algorithm was presented in [14] while our work was under review. While the algorithm presented in [14] uses a different control surface to the PS-CMA described above, the operation is remarkably similar. The only significant difference between the two algorithms is the initialisation procedure described in section 4.4, which mitigates the possibility of singular mal-convergence. To compare the performance of the two algorithms, we have simulated the back-to-back performance of both algorithms after a polarization rotation. The simulation was identical to that previously described for Figure.

We note from Figure that while the minimum Q-factor penalty of the equalisers is broadly similar in the optimum case, the algorithm described in [14] (Johannisson et al.) suffers from singular mal-convergence resulting in a high Q-factor penalty. A high penalty is seen for values of 9 of ±n/2 and ±3n/2, which correspond to angles whereby the energy of each signal polarization is evenly distributed onto the two receiver polarizations. This result is in agreement with the previous analysis of the performance of the PS-CMA with and without the initialisation algorithm presented in Figure and demonstrates the improvement in robustness which may be achieved with the initialisation algorithm.

3. PHASE AND POLARIZATION DIVERSE COHERENT RECEIVER

The phase and polarization diverse coherent receiver (shown in Figure 2.2) consists of three main stages: polarization splitting; phase diverse coupling and detection. In the first stage, the input signal and local oscillator are split into orthogonal polarizations by a pair of polarization beam splitters. A pair of polarization controllers are used to align the local oscillator polarizations with those from the input signal. This will ensure the maximum possible interference in the mixing stage. Signal - LO coupling is performed by a pair of 90° optical hybrids, which couple together local oscillator and signal for each polarization, and have a pair of outputs in quadrature. The four optical fields are then detected individually. Detection is normally performed with *P-I-N* photodiodes, either in single ended [23] or balanced configurations [24]. Photodiodes have an amplitude response of the form / a $|E|^2$, where I is the photocurrent and E is the incident electrical field [25]. It is the square- law response of the photodiodes which mixes the signal and LO fields together and enables coherent detection. When using single-ended detection, the local oscillator must be in the region of 20 dB

International Journal of Ethics in Engineering & Management Education
Website: www.ijeee.in (ISSN: 2348-4748, Volume 9, Issue 8, August 2022)

higher than the signal input [26]. This effectively linearises the response of the photodiode by reducing the relative contribution of the direct-detection of the signal to the overall photocurrent. While this approach simplifies the receiver somewhat and reduces the component cost, the ratio of signal to LO power is a balance of penalties due to direct-detection of the signal and penalties due to the relative intensity noise (RIN) of the local oscillator.

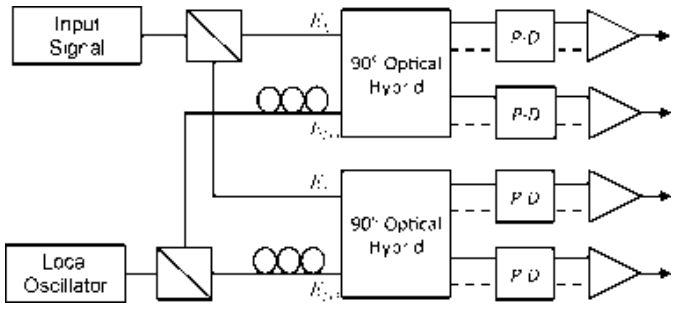

Figure 4- Phase and polarization diverse coherent receiver. Dashed lines show signals required only when balanced detection is used.

The first vector on the right hand side of the equation represents the part of the four photocurrents which are due to coherent detection. The second vector on the right hand side of the equation represents the current due to direct-detection. By making the local oscillator in the region of 20 dB more powerful than the signal, we can minimise the relative magnitude of the directly-detected signal terms (which are not constant power).

To overcome the constraints imposed on signal-LO power ratios, balanced photodetection is often employed for coherent optical receivers. In this scenario, an 8 port optical hybrid is used, with a 180° phase shift between each quadrature pair. The pairs of outputs are then differentially amplified to eliminate the direct-detection components in the signal. The 8 output ports of the hybrid are given.

3.1. Local Oscillator Phase and Frequency Locking

During the mixing process, we are effectively downconverting the modulated carrier to a baseband equivalent, albeit one which is still modulated onto the intensity of an optical carrier (before photodetection). In a homodyne system, we would mix the signal with an LO with the same frequency and phase. This process requires locking the LO phase to the optical carrier, requiring some form of feedback loop and phase control. While some optical homodyne methods provide a relatively accurate and robust solution, all solutions of this type require a high degree of optical complexity, involving expensive and sensitive components. A more favourable method of downconversion is to have a free-running local oscillator and recover the carrier frequency and phase digitally. When the intermediate frequency is less than the symbol rate, this is known as intradyning [27]. This allows lower optical complexity and the use of cheaper components, and can be combined with some form of coarse frequency control of the local oscillator to ensure that the system is able to lock continuously for many hours.

3.2. Analogue to Digital Conversion

After amplification, the four analogue electrical signals are digitised. For simplicity and performance in signal processing, it is convenient to have 2 samples per symbol. This rate of oversampling is not strictly necessary, but reduces the constraints on the required anti-aliasing filters [28] and enables compensation of a larger range of intradyne frequency offset. As these ADCs must operate in the region of 50 GSa/s, performance of these components is critical. Both the number of bits of resolution and timing jitter introduce uncertainty into the digitised signal. The jitter (or clock phase noise) reduces the accuracy of each sample, while the number of bits per sample determines the maximum accuracy of each sample. A metric of performance for ADCs is therefore the effective number of bits (ENOB), which accounts for both jitter and quantisation noise and models the effect of both as AWGN resulting in a noise floor of 6dB SNR per effective bit of resolution [29].

3.3. Digital Signal Processing Algorithms for Coherent Detection

After detection, the received signals are digitised, and then processed to compensate for distortion and impairments. While none of the functionalities provided by DSP are strictly necessary for some kind of transmission to be achieved (although not used when coherent detection was proposed in the 1980s [3], [42], sophisticated DSP was considered an important advantage in the resurgence of coherent optical communications in the 2000s [43], [44]), the increase in performance and the reduction in constraints for the design of systems provided by DSP ensure that they are an extremely attractive proposition. The signal flow model of the DSP used in the coherent communication systems in this thesis is provided in Figure 2.11. It should be noted however, that as all of these functional blocks other than the decision circuit are linear, the order of the blocks may be interchanged, and this ordering is simply one possible implementation.

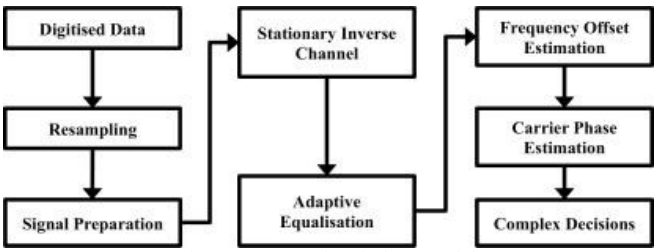

Figure 5 - DSP Signal Flow Model

3.3.1. Resampling

When asynchronous sampling is used, the digitised data is first resampled to a rate of two samples per symbol. When offline processing is used, this may be performed with a relatively simple upsample-filter-decimate algorithm. As this requires *a-priori* knowledge of the symbol rate, this is not an

International Journal of Ethics in Engineering & Management Education
Website: www.ijeee.in (ISSN: 2348-4748, Volume 9, Issue 8, August 2022)

approach that is possible to implement in hardware. The most commonly used method of digital clock recovery is the use of an interpolating filter which is sampled at a rate determined by a nonlinear timing error detector such as the Gardner loop.

3.3.2. Signal Preparation

The signal is then prepared for processing in a number of ways. The four signals must be de-skewed to compensate for the relative differences in optical path lengths inside the receiver. Any DC component of the signals must be removed to compensate for signal components which are artefacts of the receiver structure and not present in the optical spectrum. The signals are then normalised individually, such that each polarization has unit mean power. This simplifies much of the signal processing performed later and ensures that different electrical powers (due to differences in the gain of the photodetectors and amplifiers used for each of the four signals) are compensated for.

2.3.3 Stationary Inverse Channel

Due to the ability of coherent receivers to capture the full optical field, impairments due to the nature of the channel may be compensated. A major linear impairment due to the nature of optical fibre is chromatic dispersion (CD), whereby different wavelengths of light have different group velocities in the fibre. This effect may be considered as the combination of bulk material dispersion which is due to the properties of the silica which is used to make fibres, and waveguide dispersion which is due to the geometry of the fibre waveguide. As this effect is stationary, we can simply perform linear filtering with the inverse transfer function of that of the fibre. This filtering may be performed either in the frequency domain, or the time domain.

3.4. Adaptive Equalization Algorithms

Adaptive equalisation in coherent communications is most often performed with adaptive FIR filtering. These filters have been developed from the pioneering work of Bussgang [46] and Sato [47]. These equalisers are desirable as they are relatively simple to design, robust, and may be used with complex baseband signals by making the filter coefficients and signals complex. The most commonly used class of equaliser - the Bussgang equaliser - has an essential structure as described in Figure 2.12. It consists of three major parts: an FIR filter to implement the inverse channel, a memoryless non-linearity which estimates how far the filter is from the desired response, and an update algorithm which determines new filter coefficients based upon the old coefficients, the estimated position on the error surface, and the input signal to the filter.

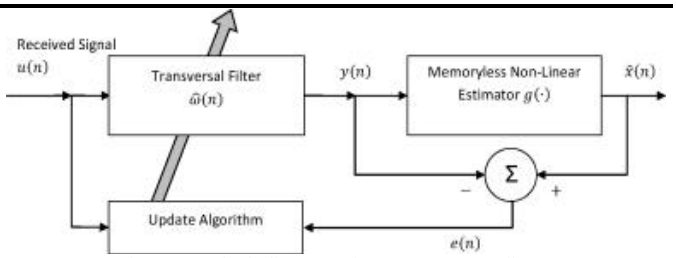

Figure 6 - Block diagram of a Bussgang equaliser.

3.5. MIMO Processing with Bussgang Equalisers

With coherent polarization multiplexed communication, the equaliser structure used to separate the two incoming polarizations (which are constantly rotating stochastically on the Poincare sphere) is very similar to that used in MIMO wireless systems. The filter structure used is known as a four-filter butterfly structure (Figure 2.13). Each output is an arbitrary combination of the input signals, thus enabling both deconvolution of the signal from the channel, and separation of the two source signals.

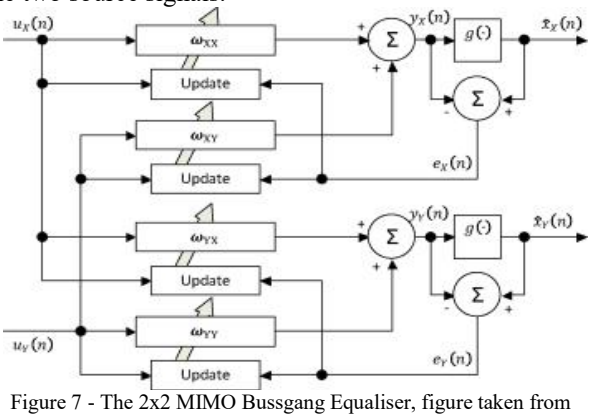

Figure 7 - The 2x2 MIMO Bussgang Equaliser, figure taken from

4. EXPERIMENTAL ANALYSIS OF DIGITAL BACKPROPAGATION

Coherent detection with receiver based digital signal processing (DSP) has recently enabled the mitigation of fibre nonlinear effects. We investigate the performance benefits available from the backpropagation algorithm for dual-polarization quadrature phase shift keying (DP-QPSK) and 16-state quadrature amplitude modulation (DP-QAM16). The performance of the receiver using a digital backpropagation algorithm with varying nonlinear step size is characterized to determine an upper bound on the suppression of intra-channel nonlinearities in a single-channel system. The results show that for the system under investigation DP- QPSK and DP-QAM16 have maximum step sizes for optimal performance of 160 km and 80 km respectively. Whilst the optimal launch power is increased by 2 dB and 2.5 dB for DP-QPSK and DP-QAM16 respectively, the Q-factor is correspondingly increased by 1.6 dB and 1 dB, highlighting the importance of studying nonlinear compensation for higher level modulation formats.

International Journal of Ethics in Engineering & Management Education
Website: www.ijeee.in (ISSN: 2348-4748, Volume 9, Issue 8, August 2022)

4.1. Experimental Transmission Setup

To characterise the functionality of our digital coherent receiver with nonlinearity compensation, we performed a set of transmission experiments to examine the effects of linear and nonlinear impairments. A particular focus was to investigate the effectiveness of nonlinear compensation techniques for DP-QPSK and DP-QAM16 modulation formats and the impact of varying DSP complexity on the transmission performance. The optical signals were transmitted multiple times through a singlespan recirculating fibre loop, followed by coherent detection, digitization and offline digital signal processing, as shown in Figure 3.1. The loop consisted of 80.2 km SMF fibre with an overall chromatic dispersion of 1347 ps/nm and loss of 15.4 dB. The experimental procedure was similar to that described.

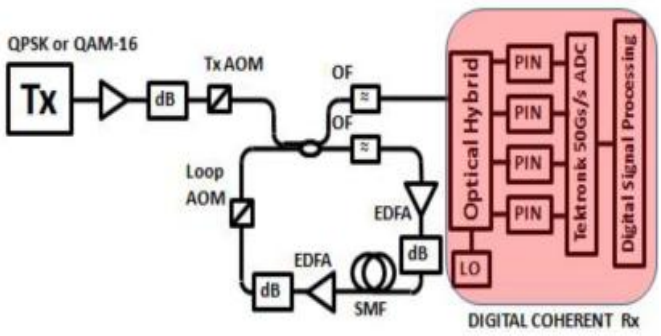

Figure 8 - Recirculating loop setup used for transmission experiments, with optical front end of the phase and polarization diverse digital coherent receiver.

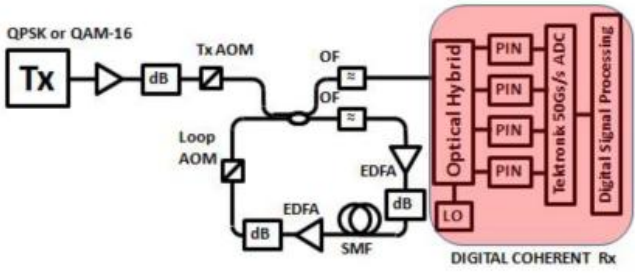

Figure 9 - Transmitter structure for DP-QPSK, with optional QAM16 stage highlighted. Inset: optical eye-diagrams at the output of the transmitter for DP-QPSK (top), and DP-QAM16 (bottom).

The polarization-multiplexed QPSK signal was generated using an I-Q modulator, which was driven over $2V_n$ with respect to the minimum bias point of its transfer function. For the data two decorrelated 2^{12} PRBS sequences were used from the output of the pulse pattern generator (PPG), which were subsequently amplified to 7 V_{p-p} ($2V_n$) to separately drive the I and Q arms of the modulator. The transmitter DFB laser linewidth, wavelength and output optical power were 1 MHz, 1554 nm and 8 dBm, respectively. To emulate polarization multiplexing we used a passive delay-line fibre interferometer, where two single polarization QPSK signals were again decorrelated, time and amplitude aligned and finally recombined via a polarization beam splitter (PBS) as shown in Figure.

To synthesise a DP-QAM16 signal, we employed a recently developed method based on the interferometric optical processing of a QPSK signal, developed by S. Makovejs [60]. To aid carrier phase estimation, an external cavity laser (ECL) with a linewidth of 100 kHz was used in the QAM16 transmitter. The initial QPSK signal was launched into a phase-stabilised fibre interferometer, where the two signals are decorrelated, time-aligned and attenuated with respect to each other by 6 dB (highlighted, Figure 3.2). The phase between two arms was set to 90° and maintained utilizing a feedback circuit. For the feedback circuit we used a ditherless bias control circuit; alternatively, a circuit design described in [105] may be used. Even though this method cannot be used to independently modulate different streams of data, this can be used to investigate transmission performance of DP-QAM16 signals. In addition, this generation method allows suppression of the transfer of noise between the electrical and optical domains in the transmitter, owing to the nonlinear transfer function of the modulator. Polarization multiplexing emulation was performed as in the DP-QPSK case.

3.4 *DP-QPSK Transmission Results*

To examine the variation of system performance with various implementations of digital backpropagation, we performed experiments with DP-QPSK near to the maximum reach without nonlinearity compensating DSP. Algorithm performance was examined over 97 spans (7780 km). As this distance is close to maximum reach, both nonlinear effects and the possible benefits of nonlinearity compensation are more significant than for shorter distances. A symbol rate of 10.7 GBd was chosen to exploit the full receiver bandwidth when using T/2 sampling for processing. The digital backpropagation algorithm was then investigated in terms of both the nonlinear step size and the use of both Wiener and Wiener-Hammerstein models.

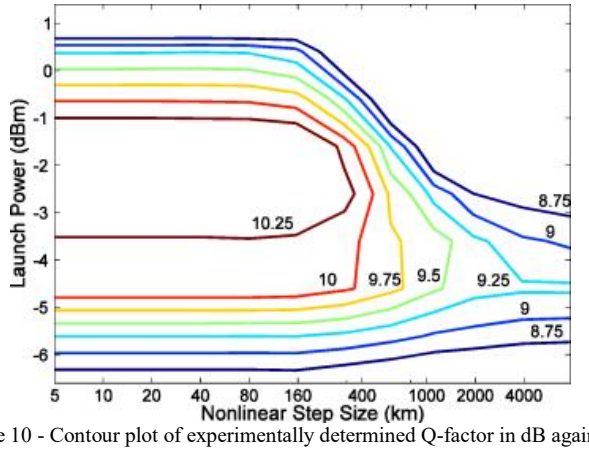

Figure 10 - Contour plot of experimentally determined Q-factor in dB against launch power and nonlinear step-size for Wiener cascade compensation of 97 spans transmission DP-QPSK at 10.7 GBd. Nonlinear step-size of a single span lies at 80.2 km.

International Journal of Ethics in Engineering & Management Education
Website: www.ijeee.in (ISSN: 2348-4748, Volume 9, Issue 8, August 2022)

The performance of the Wiener cascade model backpropagation was experimentally characterised for DP-QPSK and the results shown in Figure 3.3. Q-factor in dB is plotted as a contour graph against nonlinear step size in km on the horizontal axis and launch power in dBm on the vertical axis.

In Figure 3.3 we observe that for lower powers, performance is limited by the accumulated optical noise. For launch powers of below -5 dBm there is an insignificant improvement in performance for either modulation format with any step size. As launch power is increased, we note that an improvement in performance is available for reduced step sizes up to 160 km. The optimum launch power is improved by some 2 dB, from approximately -4.5 dBm to approximately -2.5 dBm. The benefits available with decreasing nonlinear step-size become saturated at 160 km. It is noted that while the improvement in maximum Q-factor may be modest (in the region of 1.5 dB), the increase in input dynamic range (that is, the range of launch powers for which the BER is less than the FEC limit) is more dramatic: approximately 4 dB.

4. POLARIZATION SWITCHED QPSK: THEORY AND DIGITAL EQUALISATION

Coherent detection in combination with digital signal processing has recently enabled significant progress in the capacity of optical communications systems. This improvement has enabled detection of optimum power-constrained modulation formats for optical signals in four dimensions. The increased noise tolerance of these modulation formats results in superior transmission performance which may be considered as preferable alternative to digital nonlinearity compensation, as the complexity of implementation is much lower. In this chapter, we investigate digital post-processing of one such modulation format: polarization-switched quadrature phase shift keying (PS-QPSK). Coding schemes, equalisation and WDM sensitivity are analysed, and a novel equalisation algorithm investigated. The proposed algorithm, which includes both blind initialisation and adaptation of the equaliser, is found to be insensitive to the input polarization state and demonstrates highly robust convergence in the presence of PDL, DGD and polarization rotation.

Polarization and phase diverse coherent detection with digital signal processing has become an essential technique for mitigating fibre transmission impairments and therefore increasing capacity [109]. The basis of polarization and phase diverse coherent detection is that the in-phase and quadrature components of the two orthogonal polarizations are detected, corresponding to all four dimensions of the incoming optical field [104]. As all four dimensions of the field are detected, transmission impairments such as chromatic dispersion (CD) and polarization mode dispersion (PMD) may be compensated [10]. Recently, much research has been performed into the compensation of self phase modulation (SPM) in order to gain improvements in performance of 1 or 2 dB at great computational cost [12], [63], [110].

While the detection of all four dimensions of the incoming optical field has enabled mitigation of transmission impairments, it has also enabled the use of high-level modulation formats such as quadrature phase shift keying (QPSK) [18] and 16-state quadrature amplitude modulation (QAM16) [100]. These modulation formats are most commonly transmitted on two orthogonal linear polarizations, doubling the achievable spectral efficiency. This set of modulation formats are often denoted as dual-polarization (DP-) or polarization (division) multiplexed (PDM-; PM-; or PolMux-).

Recently, research has been performed into determining the optimum modulation format in four dimensions, given that we have the ability to detect and digitally process all four dimensions of the transmitted optical field [111]. Previous proposals have focused on optimal constellations for the power constrained case [34], with some research being performed into using the extra capacity afforded by using an optimal 24-state constellation as coding overhead [112]. More recently, research into the performance of PS-QPSK in transmission has entered the literature. While this may seem to run against the trend for higher levels of modulation and more dense constellations, it may be noted that in industry there is still a demand for highly robust transmission at the expense of spectral efficiency for ultra long-haul applications [113], [114]. Despite the recent interest in PS-QPSK modulation, DSP algorithms specifically designed for PS-QPSK were published only while the algorithm presented in this chapter [13] was in peer review [14] and shortly after publication [115]. Research prior to this focusing on transmission performance of PS-QPSK over uncompensated links [116] used an equaliser utilising a training sequence. The work presented in [117] examined the performance of PS-QPSK over dispersion managed links, did not discuss equalisation. The work presented in these papers [116], [117] indicates that PS-QPSK modulation offers a significant advantage over DP-QPSK in transmission at 112 Gb/s.

5. GENERATION AND LONG-HAUL TRANSMISSION OF POLARIZATION-SWITCHED QPSK at 42.9 Gb/s

In this section, we show interestingly era and transmission of polarization-exchanged QPSK (PS-QPSK) signals at 42.9 Gb/s. Whole deal transmission of PS-QPSK is tentatively explored in a recycling circle and contrasted and transmission of double polarization QPSK (DP-QPSK) at 42.9 Gb/s per channel. A lessening in the required OSNR of 0.7 dB was found at a BER of 3.8x10-3, bringing about an expansion in most extreme range of more than 30% for a WDM framework working on a 50 GHz recurrence lattice. The most extreme compass of 13640 km for WDM PS-QPSK is, to the best of our insight, the longest separation reported for 40 Gb/s WDM transmission, over an uncompensated connection, with standard fiber and intensification.

Intelligible discovery, consolidated with computerized signal

International Journal of Ethics in Engineering & Management Education
Website: www.ijeee.in (ISSN: 2348-4748, Volume 9, Issue 8, August 2022)

handling (DSP), has prompted late increments in limit [109], reach [123], and phantom proficiency [124]. While much research has been committed to producing, preparing and transmitting frightfully effective regulation organizations, for example, abnormal state quadrature plentifulness tweak (QAM) [100], these balance arranges depend on a consistent 4-dimensional cross section group of stars configuration. In any case, it has been as of late demonstrated that these tweak configurations are not ideal for the optical divert as far as the asymptotic force proficiency [111], and some work has been embraced to decide the ideal balance position for a 4-dimensional added substance White Gaussian commotion channel [34], [111].

This exploration has prompted an assortment of new balance configurations being proposed, with different degrees of many-sided quality and trouble of acknowledgment. A configuration which has pulled in hobby is polarization-exchanged quadrature stage shift keying (PS-QPSK) [14], [34], [111], [116], [117], [125]. This arrangement transmits an image, on one of two orthogonal polarizations, with one of four just as separated stage levels from a QPSK heavenly body, such that the subsequent image conveys 3 bits of data.

This is delineated with a couple of test heavenly bodies in Figure 5.1, where blue focuses signify a QPSK image which has been transmitted on the x-polarization, while red dabs mean a QPSK image transmitted on the y-polarization. Whilst this regulation organization has a lower accessible ghastly proficiency than DP-QPSK, the addition in clamor resilience is as much as 1.76 dB [111] at equivalent piece rates and asymptotically high optical sign to commotion proportion (OSNR). For the bit-blunder rate (BER) values joined with present day forward mistake adjustment (FEC) codes, a change of 1 dB at a BER of 10-3 and of 0.55 dB at a BER of 10-2 is hypothetically achievable. Because of the huge advantage in clamor resistance over DP-QPSK which has turned into the standard tweak design for 100 GbE innovation [11], there has been some interest as of late in the transmission properties of PS-QPSK [116], [117], [125]. For this exploration we utilized an effectively feasible procedure to tentatively produce PS-QPSK, without the utilization of either a four-dimensional modulator or specially crafted photonic incorporated circuits. PS-QPSK was then described for whole deal WDM transmission and contrasted with DP-QPSK.

5.1. PS-QPSK Generation and Experimental Setup

To assess the achievable advantages of utilizing the PS-QPSK balance group over DP-QPSK, we initially measured the OSNR resilience and most extreme span of both balance positions. The analyses were directed at the steady piece rate of 42.9 Gb/s, relating to 14.3 Gbaud for PS-QPSK and 10.725 Gbaud for DP-QPSK. In WDM transmission, both configurations were transmitted over a 50 GHz recurrence matrix, with phantom productivity of 0.8 b/s/Hz in both cases.

The PS-QPSK arrangement was created as takes after (Figure 5.2(b)). Initial a triple Mach-Zehnder modulator (MZM) was utilized to regulate CW light from an outside depression laser (ECL) to create a solitary polarization QPSK grouping. The connected information example was a pseudo-arbitrary piece arrangement (PRBS) of length 215-1, where the PRBS was decorrelated by half of the example length between the in-stage and quadrature signal parts. Polarization exchanging was then connected to the sign by latently 50:50 part the QPSK signal and force adjusting every arm, image synchronously, with two MZMs. The two force modulators were driven by DATA and DATA individually from the example generator. The impact of this design being that stand out force modulator was transmitting amid every image period. The two arms were then tuned to be orthogonally energized utilizing polarization controllers, before entering a polarization shaft combiner. Any remaining image timing contrast, because of diverse way lengths in the polarization exchanging stage, was remunerated with a variable optical postponement line in one arm.

DP-QPSK was produced utilizing a comparable strategy aside from that, after the 50:50 splitter, the QPSK sign was polarization-multiplexed by decorrelating the sign polarizations in every arm of an inactive postponement line stage (Figure 5.2(a)). The successful postponement between the QPSK signals in every polarization was 24 images.

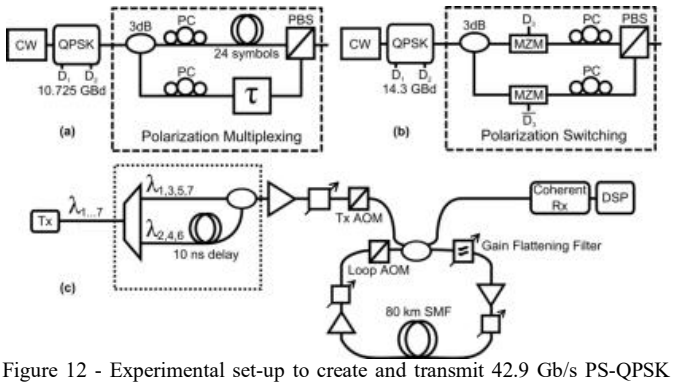

Figure 12 - Experimental set-up to create and transmit 42.9 Gb/s PS-QPSK (14.3 Gbaud) and DP-QPSK (10.725 Gbaud).

So as to create a 7-channel WDM brush, two changes to the above setup were presented. Firstly, a 50 GHz WDM brush was made by joining CW light from six temperature-and current-controlled DFB lasers. An ECL with a linewidth of 100 kHz was utilized for the focal channel. The brush was mass regulated, and an interleaver with a channel dividing of 50 GHz was utilized to independent exchange channels, which were then decorrelated by 10 ns before being recombined with a 3-dB fiber coupler, as portrayed in (A H Gnauck et al. 2011).

CONCLUSION

In this paper we describe proposed future research topics in the field of DSP algorithms for coherent detection. First, we

discuss performance bounds on the capability of digital backpropagation for coherent systems. We then discuss DSP algorithms for modulation formats which are optimal in four dimensions. Extending the filter initialisation algorithm presented in chapter 4 to conventional modulation formats such as DP-QPSK and DP-QAM16 is then proposed. Finally we draw conclusions on each part of the research, and on the larger conclusions to be drawn from this research project as a whole.

REFERENCES

[1] K. C. Kao and G. a Hockham, "Dielectric-fibre surface waveguides for optical frequencies," *IEE Proceedings J Optoelectronics,* vol. 133, no. 3, p. 191, 1986.

[2] R. S. Vodhanel, A. F. Elrefaie, M. Z. Iqbal, R. E. Wagner, J. L. Gimlett, and S. Tsuji, "Performance of directly modulated DFB lasers in 10-Gb/s ASK, FSK, and DPSK lightwave systems," *Lightwave Technology, Journal of,* vol. 8, no. 9, pp. 1379-1386, 1990.

[3] K. Kikuchi, T. Okoshi, and J. Kitano, "Measurement of bit-error rate of heterodyne-type optical communication system-A simulation experiment," *Quantum Electronics, IEEE Journal of,* vol. 17, no. 12, pp. 2266-2267, 1981.

[4] R. J. Mears, L. Reekie, I. M. Jauncey, and D. N. Payne, "Low-noise erbium- doped fibre amplifier operating at 1.54pm," *Electronics Letters,* vol. 23, no. 19, p. 1026, 1987.

[5] C. A. Brackett, "Dense wavelength division multiplexing networks: principles and applications," *Selected Areas in Communications, TEEE Journal on*, vol. 8, no. 6, pp. 948-964, 1990.

[6] P. J. Winzer and R. J. Essiambre, "Advanced optical modulation formats," *Proceedings of the IEEE,* vol. 94, no. 5, pp. 952-985, 2006.

[7] J. M. Kahn and K.-P. Ho, "Spectral Efficiency Limits and Modulation/Detection Techniques for DWDM Systems," *TEEE Journal of Selected Topics in Quantum Electronics,* vol. 10, no. 2, pp. 259-272, Mar. 2004.

[8] H. Sun, K. T. Wu, and K. Roberts, "Real-time measurements of a 40 Gb/s coherent system," *Optics Express,* vol. 16, no. 2, pp. 873-879, 2008.

[9] E. Ip, A. P. T. Lau, D. J. F. Barros, and J. M. Kahn, "Coherent detection in optical fiber systems," *Optics Express,* vol. 16, no. 2, pp. 753-791, 2008.

[10] S. J. Savory, "Digital filters for coherent optical receivers," *Optics Express,* vol. 16, no. 2, pp. 804-817, 2008.

[11] "Implementation Agreement for Integrated Dual Polarization Intradyne Coherent Receivers," *Optical Tnternetworking Forum*, 2010. [Online]. Available: www.oiforum.com/public/documents/OIF_DPC_RX-01.0.pdf.

[12] D. S. Millar et al., "Mitigation of Fiber Nonlinearity Using a Digital Coherent Receiver," *Selected Topics in Quantum Electronics, Journal of,* vol. 16, no. 5, pp. 1217-1226, 2010.